Scientific Research Publishing

Advances in Remote Sensing, 2024, 13, 41-71
https://www.scirp.org/journal/ars
ISSN Online: 2169-2688
ISSN Print: 2169-267X

Satellite Multi-Temporal Data and Cropping Pattern Approach for Green Gram Crop Management in the Lower Midland Zone IV and V in Kenya

Kalekye Hilda Manzi[1*], Shadrack Ngene[2], Joseph P. Gweyi-Onyango[1]

[1]Department of Agriculture Science and Technology, School of Agriculture and Enterprise Development, Kenyatta University, Nairobi, Kenya
[2]Kenya Wildlife Service, Spatial Ecology and Biodiversity Monitoring, Nairobi, Kenya
Email: *manzikye@gmail.com

How to cite this paper: Manzi, K.H., Ngene, S. and Gweyi-Onyango, J.P. (2024) Satellite Multi-Temporal Data and Cropping Pattern Approach for Green Gram Crop Management in the Lower Midland Zone IV and V in Kenya. *Advances in Remote Sensing*, **13**, 41-71.
https://doi.org/10.4236/ars.2024.132003

Received: May 24, 2024
Accepted: June 27, 2024
Published: June 30, 2024

Abstract

Creation of a spectral signature reflectance data, which aids in the identification of the crops is important in determining size and location crop fields. Therefore, we developed a spectral signature reflectance for the vegetative stage of the green gram (*Vigna. radiata* L.) over 5 years (2020, 2018, 2017, 2015, and 2013) for agroecological zone IV and V in Kenya. The years chosen were those whose satellite resolution data was available for the vegetative stage of crop growth in the short rain season (October, November, December (OND)). We used Landsat 8 OLI satellite imagery in this study. Cropping pattern data for the study area were evaluated by calculating the Top of Atmosphere reflectance. Farms geo-referencing, along with field data collection, was undertaken to extract Top of Atmosphere reflectance for bands 2, 3, 4 and 7. We also carried a spectral similarity assessment on the various cropping patterns. The spectral reflectance ranged from 0.07696 - 0.09632, 0.07466 - 0.09467, 0.0704047 - 0.12188,0.19822 - 0.24387, 0.19269 - 0.26900, and 0.11354 - 0.20815 for bands 2, 3, 4, 5, 6, and 7 for green gram, respectively. The results showed a dissimilarity among the various cropping patterns. The lowest dissimilarity index was 0.027 for the maize (*Zea mays* L.) bean (*Phaseolus vulgaris*) versus the maize-pigeon pea (*Cajanus cajan*) crop, while the highest dissimilarity index was 0.443 for the maize bean versus the maize bean and cowpea cropping patterns. High crop dissimilarities experienced across the cropping pattern through these spectral reflectance values confirm that the green gram was potentially identifiable. The results can be used in crop type identification in agroecological lower midland zone IV and V for mung bean

management. This study therefore suggests that use of reflectance data in remote sensing of agricultural ecosystems would aid in planning, management, and crop allocation to different ecozones.

Keywords

Multi-Temporal, Cropping Patterns, Spectral Signatures, Landsat 8, Crop, Identification

1. Introduction

Smallholder farms in Kenya face numerous challenges in data collection due to the fragmented farm holding, variability in crop types and farming practices [1]. Green gram (*Vigna radiata* L.) crops provide several management issues, particularly in places with fragmented landscapes and smallholder farms. Traditional crop monitoring and management approaches frequently fall short due to the labor-intensive nature of ground surveys, unpredictability in crop growth stages, and a lack of timely and accurate data. Additionally, there is lack the resources to systematically gather and analyze agricultural data, leading to gaps in information that are critical for making informed decisions about crop management, pest control, and yield optimization [2]. Smallholder farms are usually subdivided into parcels whose boundaries are hard to distinguish and/or clearly delineate [3]. Spatial information on agricultural fields is important for appropriate understanding, planning, and management of crop growth conditions. This information is essential to improve crop yield prediction, provide crop management advice, allocate resources, and monitor the effectiveness of development interventions [4]. Forecasting and monitoring agricultural production is a very crucial part of food demand and overall food security. Remote sensing tools have been widely used in crop area estimation, crop type identification, and yield estimation. Standard methods of estimation of area under crop have relied on techniques such as area statistical frame studies [5]. These are some of the field-based survey studies that can take long time and resources, especially when dealing with small-holder farms [6]. Furthermore, knowledge sharing, and dynamics are important in decision-making and academic studies related to the green gram.

Earth observation data coupled with good cropping pattern training data has revolutionized crop identification, making it easier to understand the spatial distribution of crops [7]. Advances in crop monitoring using remote sensing data take advantage of indices and biophysical parameters such as normalized difference vegetable index (NDVI) and Leaf Area Index (LAI) and photosynthetically active radiation (FAPAR), respectively to achieve the final goal [7]. The forementioned variables were obtained from space measurement in the visible and near-infrared bands. [8] described a method for multidate supervised classification of normalized difference vegetation index (NDVI) using Landsat 8 data for crop

diversity mapping. In their research, they concluded that remote sensing could solve complex problems in tropical developing countries.

The importance of satellite image-derived vegetation indices for crop condition assessment such as normalized difference vegetation (NDVI), land surface water index (LSWI), Temperature Vegetation Dryness Index (TVDI), soil adjusted vegetation index (SAVI), among others to be very crucial in the assessment of crop development state has been highlighted [9]. In addition, the research documents indicate the use of remote sensing to estimate crop area and crop situation as a result of water stress, pests infestation and disease infections. [10] pointed out the confusion that occurs between vegetation and cropland as a major source of error in remote sensing-based crop mapping, especially with low-resolution imagery and in areas with complicated crop-planting patterns. The variability in cropland can be reduced if satellite data cover key phenological phases of the crop since surface reflectance changes with the growth stages of the crops [10]. The use of hyperspectral images cannot be overemphasized since it has made significant strides in the development of crop spectral library lately. A study by [11] showcases promising results in the discrimination against rice (*Oryza sativa*), sugarcane (*Saccharum officinarum*), pepper, and cotton (*Gossypium hirsutum*) cultivars. The research confirmed the potential of using crop reflectance with the help of spectral signatures to separate various crop cultivars. Furthermore, [11] were able to highlight the spectral similarity between rice and sugarcane, which however, presented challenges. Successes of the use of hyperspectral data in the classification and discrimination of crops and varieties have also been demonstrated [12]-[16]. The Global Hyperspectral Imaging Spectral Library of Agricultural Crops (GHISA) for Central Asia has been developed and provides insight to crop spectral libraries, [17]. The challenge of hyperspectral data is computing time, calibration, and redundancy of high data volume [18]. Other multispectral sensor data, such as sentinel-2, have been shown to provide promising results [19]-[21], where the capabilities in crop monitoring and land cover classification have been found to be very crucial. [22] showed the importance of red edge bands of sentinel-2 in vegetation analysis. Their research proved that the accuracies were much better when red edge bands were used compared to the accuracies of Landsat 8 or sentinel-2 satellite data and they recommend the combination of Landsat 8 and sentinel-2 data for improved accuracy.

The traditional approach to crop classification with remote sensing data has been based primarily on supervised and unsupervised classification techniques to map the geographic distribution of crops [23]. Remote sensing images represent features on Earth with respect to their corresponding spectral reflectance, known as a spectral [23]. Based on the same concept, two different types of crops can exhibit different spectral signatures, which can be used to distinguish them in the classification. In plant species, these differences in signature are due to their phenology, leaf orientation, and canopy structure. Multi-temporal, red, and infrared indices and their ratio indices (vegetation indices) have been used successfully to

evaluate plant phenology [24].

Green gram (*Vigna. radiata* L.) also known as mung bean, is one of important legumes among smallholder farmers in Kenya, and the consumption has significantly increased. Green gram is one of the most important legume crops in the world [25]-[27] and in Kenya, it is grown successfully in Eastern part mainly in Machakos, Kitui, Tharaka-Nithi, and Makueni counties due to its adaptability to low [28]. Machakos county located in the lower eastern parts of Kenya, leads in green gram production and this crop grows in various soil types and climatic conditions because of its ability to tolerate low soil moisture regimes [29]. The crop can grow well in various soil conditions even with limited nutrients such as phosphorus (P) [30]. This is due to the fact that green gram forms an excellent association with mycorrhiza within its rhizosphere [30], hence it plays a vital role in improving soil fertility. Smallholder farms form primary food sources in developing countries with about 90% provision capacity [31] [32] making the understanding the production of this vital crop is therefore essential for planning and monitoring food security.

To address the issues of crop identification in fragmented land parcels, the study proposes using spectral signature reflectance from multi-temporal data. Crop spectral signatures obtained from multispectral imaging at key periods are extremely valuable for crop identification, particularly during phenological cycles and spectral similarity. To improve the accuracy of this approach using Landsat 8, cultivated areas were demarcated using field survey data to determine crop patterns while also using farm parcel data. Further, throughout several years, crop spectral signature reflectance ranges were established for the same field in a specific season (short rains) and phenological stage (vegetative stage) of the phenological cycle, as well as their statistical (di)similarity. Using spectral reflectance, useful information was obtained by analyzing the temporal reflectance and spatial reflectance features of vegetation for proper crop identification.

In this study, the investigation focused on satellite data for the vegetative stage of growth around late December to mid-January to mid-late February due to delayed rains. This data set was only available on Landsat 8 and not in sentinel-2 as was anticipated. The high cloud cover in sentinel-2 generally affected the expected or anticipated crop spectral reflectance, which was execrated by the lack of data for the period of interest. The study presents a multifaceted approach in green gram growing areas in semiarid areas of agroecological zone IV and V using reflectance data and image statistics and temporal time series-based approaches in the identification of cropping patterns and spectral signature ranges for crop identification in a specific crop stage, season, and agroecological zone. The challenges of nonuniformity of coverage of ground truth data and satellite scenes and seasonal differentiation of crop groups were addressed through acquired Landsat 8 images over different years, working in a specific agroecological zone for a particular phenological stage within a growing season.

The paper is organized such that an introduction discusses the purpose of the

research and the reasoning behind it. Materials and procedures that outline the research area, techniques, and approach are then presented. The study's conclusions are presented in the upcoming chapter, along with a discussion that weighs the findings in light of prior research. The study's conclusion, which highlights the significance of the findings and offers suggestions for additional research, comes last.

2. Materials and Methods

2.1. Experimental Site

The study area was the Ikombe-Katangi ward located in the semi-arid area found in the southern region of Kenya in Machakos County (1˚16'24.55"S; 37˚40'13.30"E) (**Figure 1**). Eighty percent of this landscape is classified as semi-arid and arid lands that are highly susceptible to the effect of climate change [33]. These are part of the marginal areas of Kenya, highly vulnerable to degradation due to fragile landscapes. These semi-arid areas are characterized by fluctuating rainfall patterns that are highly erratic and unreliable. The amount of rainfall is low and characterized with very high temperatures of between 28oc to 30oc, with resultant high evapotranspiration rates [33]. The normal cropping calendar commences in mid-October, allowing most of the crops to reach physiological maturity in January. In the last 5 years, rainfall fluctuation in Ikombe-Katangi area has been very high, with rains starting in mid or end of November, causing most crops to reach physiological maturity at the end of February [33]. The area is characterized by small-holder farmers practicing mixed cropping characterized by maize (*Zea mays*), Pigeon pea (*Cajanus cajan*), beans (*Phaseolus vulgaris*), cow pea (*Vigna unguiculata*), and green grams (*Vigna radiata*) [34]. The area under investigation lies in agroclimatic

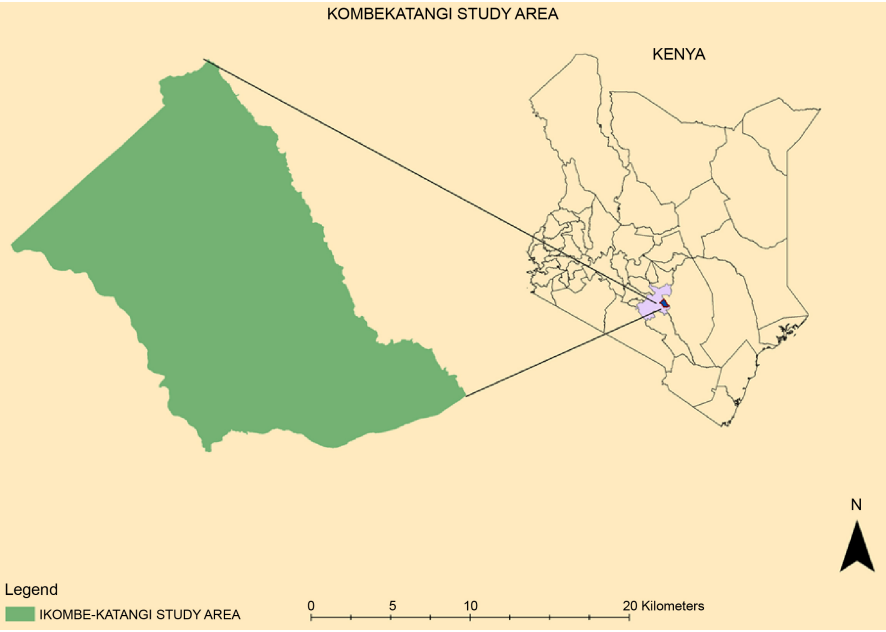

Figure 1. Map illustrating Ikombe-Katangi experimental site in Machakos County, Kenya.

zone IV with bimodal rainfall patterns [35]. The cropping calendar follows the bimodal rainfall regime with short rains (SR) occurring in the October, November, and December season, while long rains (LR) occur in March, April, and May season (Table 1). The geographical region is a plateau, which extends north and south of Machakos county with an elevation of 1700 m and covers an area of 1059 km^2. The study area receives 500 mm of rain with temperatures ranging from 22˚C to 28˚C [35]. The soil is characterized by sandy loams, with low soil organic matter due to overworking of the soils and the fragile nature of the soils in marginal areas. These soils are from base rocks such as Ferric Luvisol, Lithisols and Rhodic Ferralsols [36].

2.2. Training Data

Ground observation data for the various cropping patterns were collected in 2020 and a further socioeconomic survey was conducted to collect additional data for the cropping patterns undertaken over the preceding 10 years. The method used for data collection and setting up the farm controls was the multistage random sampling design, where a homogeneous population was generated through the elimination of farms that were not representative of the study. The experiment was done according to [37] who used multistage sampling on rice fields to select plots in the landscape that had a population of rice farmers.

This method used digitized farms within the study area for the sampling design (Figure 2). The number of farms used in this statistical design was 10,000, which is equivalent to the total number of farms in the experimental area, and this was confirmed by the field survey (Figure 2). Level 1 of the statistical sampling designs involved the elimination of irrigation farms so that only rainfed farms were considered in the study. The irrigated farms were 5% of the total farms within the study area and this resulted in n = 9500 farms available for sampling. Level 2 of the statistical sampling involved the elimination of farms that did not have any

Table 1. Phenological growth calendar for short rains (October-November-December) for the Ikombe-Katangi area.

Phenological growth stage	Month				
	October	November	December	January	February
Germination, sprouting, bud development	Mid to End of October	Early November			
Leaf development/shoot development	End of October	Early to Mid-November			
Development of vegetative plant parts, bolting		Late November	Early to late December	Early to mid-January	
Inflorescence emergence, Flowering /Pod filling			Late December	Early to mid January	
Harvesting				Late January	Mid-February to late February

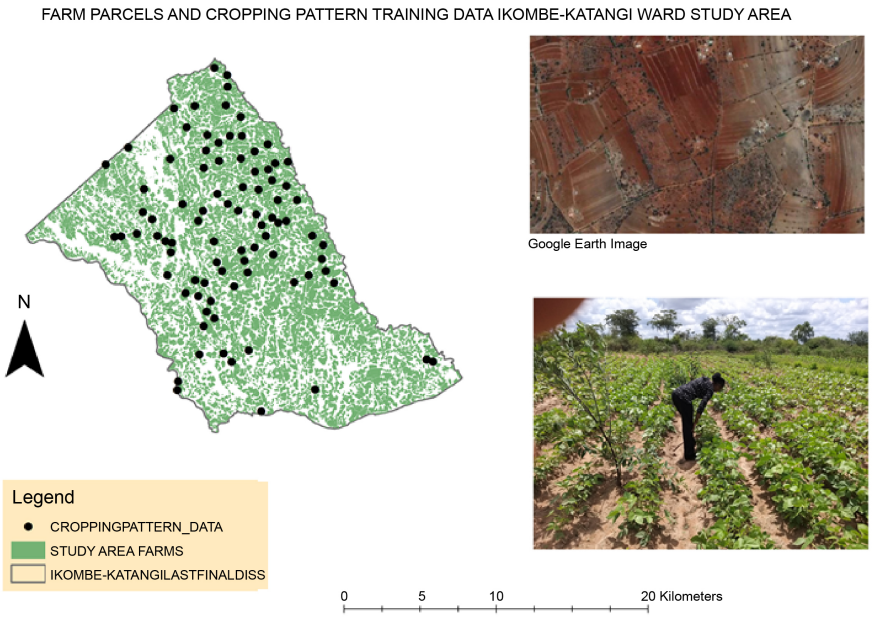

Figure 2. Parcels of farms and cropping pattern training data at Ikombe-katangi, Machakos County Kenya.

crops planted or where the crop was planted late within the planting season, for instance short rains (October, November, December (OND)). These farms were excluded from the total population of farms selected under level 1 and this resulted in the elimination of 35% of the total farms from level 1, where n = 6175. This elimination criterion was caused by the late onset of rains within the study area. At level 4 of the sampling, sub-location administrative data was used to select areas known for growing green grams in the last 5 years. Six sub-locations out of 10 were considered, resulting in n = 820 farmers. Of the 820 farms, 10% of the total number of farms were sampled for data collection. The farms sampled for cropping training were 82 farms, a bigger number than the calculated value of 23 farms. This was done to ensure a higher level of accuracy in the data collected especially in accommodating the variability in the fragmented landscapes a critical level of 10% statistic used in this study was adopted from [38] and [39]. The formula for sampling of the 10% representative farms for data collected is shown in Equation (1) below.

$$n = \frac{\left[(N)(p)(1-p)\right]}{\left[(N-1)\left(\frac{B}{C}\right)^2 + (p)(1-p)\right]} \quad (1)$$

where n is the computed sample size needed for the desired level of precision; N is the population size; p is the proportion of the population expected to choose; B is the acceptable amount of sampling error, or precision; and finally, C is the Z statistic associated with the confidence level, which is 1.96 and corresponds to the 95% level. B was set at 0.05, which is ± 10% of the true population value,

respectively. The acceptable amount of sampling error or precision was set at 0.05 or 5%. A confidence level of 1.96 corresponds to the 95% level.

where $N = 820$, $p = 0.1$, $B = 0.05$, $C = 1.96$

$n = [(820)\ (0.1)\ (1-0.5)]/[(820-1)\ (0.05/1.96)2 + (0.5)\ (1-0.5)]$

$n = [(820)\ (0.1)\ (0.5)]/[(819)\ (0.0255)2 + (0.5)\ (0.5)]$

$n = (41)/(1.56+ 0.25)$

$n = 41/1.81$

$n = 22.65 \approx 23$

2.3. Field Survey

A field survey was conducted to generate adequate data for the statistical sample design. Questionnaires were administered to collect planting information from 150 farmers. The data collected were planting season, date of planting, crops planted, varieties, cropping pattern, size of the farm, GPS coordinates of the farm including elevation data, information of agricultural and practices carried out on the farm (weeding, fertilizer application, etc.). These data sets were important in understanding changing cropping patterns on small farmland. Table 2 shows the identified cropping patterns and their frequencies as captured from the field data. Figure 3 presents training data collection points for the field survey on Landsat 8 satellite imagery used for this investigation.

2.4. Pre-Processing of Landsat 8 Satellite Imagery

The study used data from 2013, 2015, 2017, 2018 and 2020 because they represent good data with minimal or no cloud cover around the study area for the short rain period (October, November and December (OND)) rains during which green gram cultivation was carried out. [40] showed that images acquired on different dates during the crop growth period are usually required to discriminate certain

Table 2. Cropping patterns constituting different crops identified within the experimental area.

Type of cropping pattern	Cropping Pattern Key	Cropping Pattern Frequency				
		2013	2015	2017	2018	2020
Mixed Crop (MPB)	Maize, Pigeon pea and Beans	4	5	5	4	0
Mixed Crop (MG)	Maize and Green Gram	8	5	6	2	5
Mixed Crop (MB)	Maize and Beans	11	15	11	13	20
Maize	Maize	22	24	23	23	24
Green Gram	Green Gram	5	7	8	6	5
Mixed Crop (MP)	Maize and Pigeon pea	28	25	26	30	33
Mixed Crop (MC)	Maize and Cowpea	6	3	5	5	1
Mixed Crop (MPC)	Maize, Pigeon pea and Cow Pea	3	3	0	2	0
Bean	Bean	2	0	1	2	1
Mixed Crop (MCB)	Maize, Cow pea and Beans	1	1	5	3	0

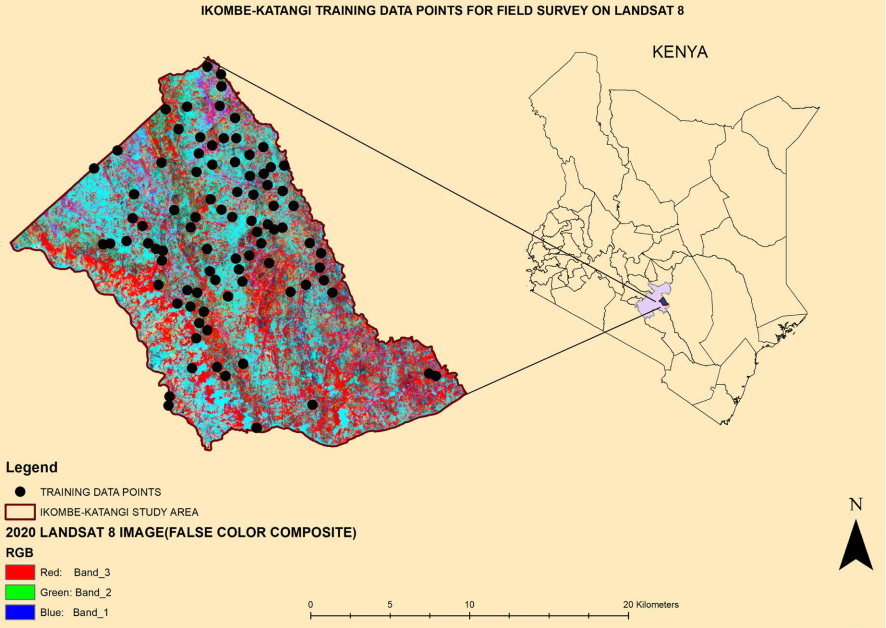

Figure 3. Training data collection points for the field survey on Landsat 8 satellite imagery.

crop types. The research used Landsat 8 data for the long rain season for 2020, 2018, 2017, 2015, and 2013 within the study area. The acquired data considered images within the same temporal resolution. In addition, the landscape vector data for this study area was acquired from Kenya's administrative ward data to aid in the extraction of the area of interest in the satellite imagery.

The collection 2 level one satellite images of the Landsat-8 OLI products that were used within the scope of this study were obtained from the website of the American Geological Service (USGS) with orthorectification and radiometric correction. The images were in the Universal Transverse Mercator (UTM) coordinate system, and geometric corrections were made to position them on 37 South and the WGS84 datum. Image enhancements such as standard deviation and histogram equalization were performed to enable features identification. Furthermore, an overlay with farm boundaries was also performed (**Figure 4**) to allow identification of cropped areas during classification. The metadata of the images were used (**Table 3**) and band selection was done as described by [41]. This study also

Table 3. Landsat 8 OLI scene satellite imagery metadata.

Landsat 8 product	Type of product	Path	Row	Date of acquisition	Cloud cover
LC08_L1TP	Collection 2 level 1	168	61	20/02/2020	1.30
LC08_L1TP	Collection 2 level 1	168	61	2018-01-29	0.02
LC08_L1TP	Collection 2 level 1	168	61	2017-12-28	0.26
LC08_L1TP	Collection 2 level 1	168	61	2015-01-05	2.48
LC08_L1TP	Collection 2 level 1	168	61	2013-11-15	3.59

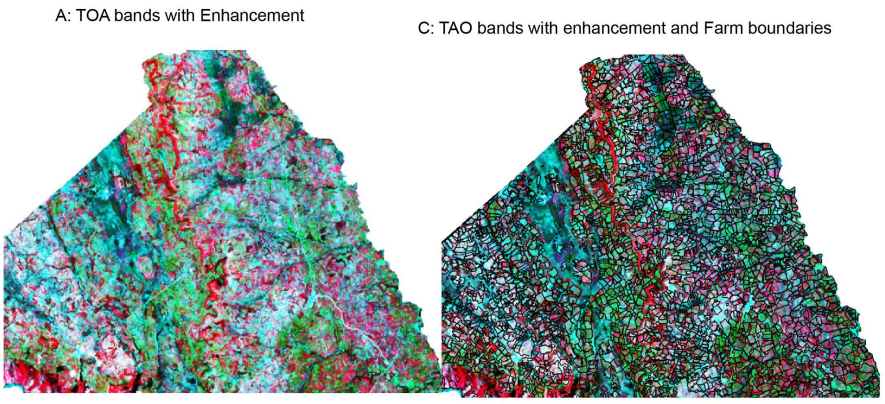

Figure 4. Image enhancement and farm boundary overlay in Ikombe-katangi, Machakos County Kenya.

relied on Landsat 8 band information to enhance a band combination for differentiation of characteristics in a classification. Band 2 was used to distinguish soil from vegetation, especially in areas where the vegetation is scattered with a low cover typical of farms in the study areas. Band 3 was used to evaluate plant vigour, while 4 and 5 assisted in vegetation classification while bands 6 and 7 were crucial in the classification of irrigated areas.

2.5. Reflectance Calculations

The uses of the Top of Atmosphere (TOA) in calculation of TOA reflectance for bands 2, 3, 4, 5, 6 and 7 which are very important in the identification of cropped area on Landsat 8 satellite imagery compared to the use of Bottom of Atmosphere (BOA) was adopted from [42]. The challenges of atmospheric correction that might accumulate errors in the BOA reflectance data required the use of TOA for a surface that is a plateau (generally flat). Landsat 8 bands 6 and 7 in the study were used in the assessment of moisture contents in soil and vegetation in order to ensure that the rainfed crops were properly identified during classification. The calculation of reflectance is crucial when creating multitemporal and/or multispatial mosaics, as it largely removes variations between these images due to sensor differences, Earth-Sun distance, and solar zenith angle (caused by different scene dates, overpass time, and latitude differences) [43]. Conversion from DN to TOA reflectance was applied in this study as suggested [44] and it is the most crucial step in producing "accurate" spectral reflectance. In this study, the retrieval performance of sentinel-2 BOA and TOA data did not produce variable significant differences. The top of atmospheric reflectance calculated by reflectance using the rescaling coefficients in the MTL file found alongside the downloaded satellite images for Landsat 8 was calculated as follows:

$$L\lambda' = M_\rho Q_{cal} + A_\rho \tag{10}$$

where:

$L\lambda'$ = TOA radiance, without correction for solar angle. Note that $\rho\lambda'$ does

not contain a correction for the sun angle;

$M\rho$ = Band-specific multiplicative rescaling factor from the metadata (REFLECTANCE_MULT_BAND_x, where x is the band number);

$A\rho$ = Band-specific additive rescaling factor from the metadata (REFLECTANCE_ADD_BAND_x, where x is the band number);

$Qcal$ = Quantized and calibrated standard product pixel values (DN).

This formula is adopted from [45].

Converting the TOA radiance to TOA reflectance:

$$\rho TOA = \frac{L\lambda' \cdot d^2 \cdot \pi}{ESUN_\lambda \cdot Cos(\theta_{SZ})} \tag{3}$$

where

$L\lambda$ = TO where d is the Earth-Sun distance, $ESUN_\lambda$ is the mean solar exoatmospheric irradiance, and θ_{SZ} is the solar zenith angle [46].

The reflectance value was performed for all five years and the data are represented in **Table 4**. In this study All cropping patterns identified from the ground observation were subjected to the Euclidean distance spectral dissim assessment by comparing all patterns against possible outcomes. The method is deterministic and looks at the shape of the wavelength [47]. Using data obtained from the field surveys ground truth data for various crop types with precise geographic locations was used for extraction of the spectral signatures (reflectance values at different wavelengths) for the identified crops at the ground truth locations [7] [48]. The Euclidean distance was calculated using the formula.

$$d(p,q) = \sqrt{\sum_{i=1}^{n} (p_i - q_i)^2} \tag{4}$$

where p_i and q_i are the reflectance values of the pixel and the reference signature at the ith wavelength, respectively [49].

Table 4. Computation of the top of atmosphere reflectance for all the cropping patterns for bands 2, 3, 4, 5, 6, and 7.

Year	Band Wavelength	Mixed Crop (MPB)	Mixed Crop (MG)	Mixed Crop (MB)	Maize	Green Gram	Mixed Crop (MP)	Mixed Crop (MC)	Mixed Crop (MPC)	Bean	Mixed Crop (MCB)
2013	0.455	0.08927	0.09586	0.09782	0.09714	0.09611	0.09523	0.09042	0.09455	0.10394	0.00000
2013	0.56	0.08397	0.09349	0.09682	0.09286	0.09467	0.09320	0.08738	0.09497	0.10117	0.00000
2013	0.655	0.11389	0.11269	0.12533	0.11367	0.12188	0.11541	0.11783	0.11799	0.12419	0.00000
2013	0.865	0.17718	0.19634	0.19709	0.17834	0.20016	0.18541	0.19077	0.18765	0.19208	0.00000
2013	1.62	0.24180	0.24705	0.27321	0.24897	0.26900	0.26013	0.26677	0.26864	0.28703	0.00000
2013	2.2	0.19331	0.19179	0.21507	0.19643	0.20815	0.20364	0.20649	0.20739	0.23309	0.00000
2015	0.455	0.08178	0.07869	0.07738	0.07785	0.07845	0.07767	0.07505	0.07827	0.00000	0.00000
2015	0.56	0.08142	0.07211	0.07469	0.07497	0.07489	0.07526	0.07280	0.07605	0.00000	0.00000
2015	0.655	0.08380	0.07236	0.08117	0.08121	0.07564	0.07716	0.06525	0.08031	0.00000	0.00000

Continued

2015	0.865	0.24936	0.19873	0.23230	0.22657	0.22178	0.23125	0.26128	0.22892	0.00000	0.00000
2015	1.62	0.22320	0.18761	0.20874	0.20457	0.19699	0.20628	0.17366	0.19619	0.00000	0.00000
2015	2.2	0.15126	0.12995	0.14266	0.14050	0.13043	0.13868	0.10051	0.13174	0.00000	0.00000
2017	0.455	0.07797	0.07567	0.07891	0.07801	0.07696	0.07651	0.07704	0.00000	0.00000	0.07734
2017	0.56	0.07738	0.07425	0.07842	0.07528	0.07466	0.07421	0.07032	0.00000	0.00000	0.07668
2017	0.655	0.09232	0.08937	0.08987	0.08499	0.08390	0.08719	0.07688	0.00000	0.00000	0.09117
2017	0.865	0.19938	0.19458	0.20790	0.19507	0.19822	0.19126	0.15944	0.00000	0.00000	0.20300
2017	1.62	0.23083	0.21366	0.22584	0.21146	0.19725	0.21912	0.19497	0.00000	0.00000	0.22754
2017	2.2	0.16924	0.15447	0.15943	0.15161	0.14430	0.15880	0.14508	0.00000	0.00000	0.16386
2018	0.455	0.08929	0.09017	0.09379	0.09033	0.09632	0.09112	0.09249	0.08673	0.08868	0.09468
2018	0.56	0.08767	0.09264	0.09586	0.08924	0.09672	0.09212	0.09578	0.08645	0.08932	0.09685
2018	0.655	0.10684	0.12070	0.12362	0.11328	0.11869	0.12156	0.12807	0.11046	0.11701	0.11856
2018	0.865	0.20444	0.21914	0.22083	0.20093	0.20667	0.21193	0.22814	0.20931	0.21768	0.21566
2018	1.62	0.23805	0.26873	0.29415	0.25914	0.26891	0.27938	0.29846	0.24534	0.26241	0.29436
2018	2.2	0.17199	0.19829	0.22210	0.19884	0.20345	0.21170	0.23097	0.18363	0.19895	0.21677
2020	0.455	0.00000	0.07989	0.07765	0.07880	0.08206	0.07922	0.00000	0.00000	0.00000	0.00000
2020	0.56	0.00000	0.07697	0.07615	0.07766	0.07916	0.07814	0.00000	0.00000	0.00000	0.00000
2020	0.655	0.00000	0.07061	0.06397	0.06949	0.07047	0.06976	0.00000	0.00000	0.00000	0.00000
2020	0.865	0.00000	0.24227	0.27798	0.26834	0.24387	0.26933	0.00000	0.00000	0.00000	0.00000
2020	1.62	0.00000	0.18978	0.18944	0.19581	0.19269	0.19582	0.00000	0.00000	0.00000	0.00000
2020	2.2	0.00000	0.11448	0.10414	0.11376	0.11354	0.11367	0.00000	0.00000	0.00000	0.00000

2.6. Land Cover Classification for the Study Area

The maximum likelihood classification classifier was used in the classification of TOA band composite image from multispectral datasets. To further improve satellite imagery, standard deviation and histogram equalization enhancements were performed using ARCGIS software (**Figure 4**) The crop pattern data was used to train the land cover classification while farm boundaries were overlaid during the classification to increase the classification accuracies as shown in **Figure 4**. The maximum likelihood classifier as documented by [50] provides good results in data-intensive environments. The crop pattern training data provided good information for the proper discrimination of the various crop classes in the study area. The critical role of training data as described by [51] cannot be overemphasized, especially where the maximum likelihood classifier is used. In this study, land-cover classification was performed to evaluate the effectiveness of crop discrimination using spectral signature ranges in the identification of green gram. Cropping pattern field data for the year 2020 was collected during the short rain season (October, November, December (OND)) and used in the classification while targeting the specific spectral signature ranges. The basis for separating one crop

from another is the assumption that each crop species has a specific spectral signature in a time series of multispectral images. This is achieved by varying the plant reflectance of different crops and a proper understanding of cropping patterns for the areas analyzed. The methodology workflow used in the classification is shown in Figure 5.

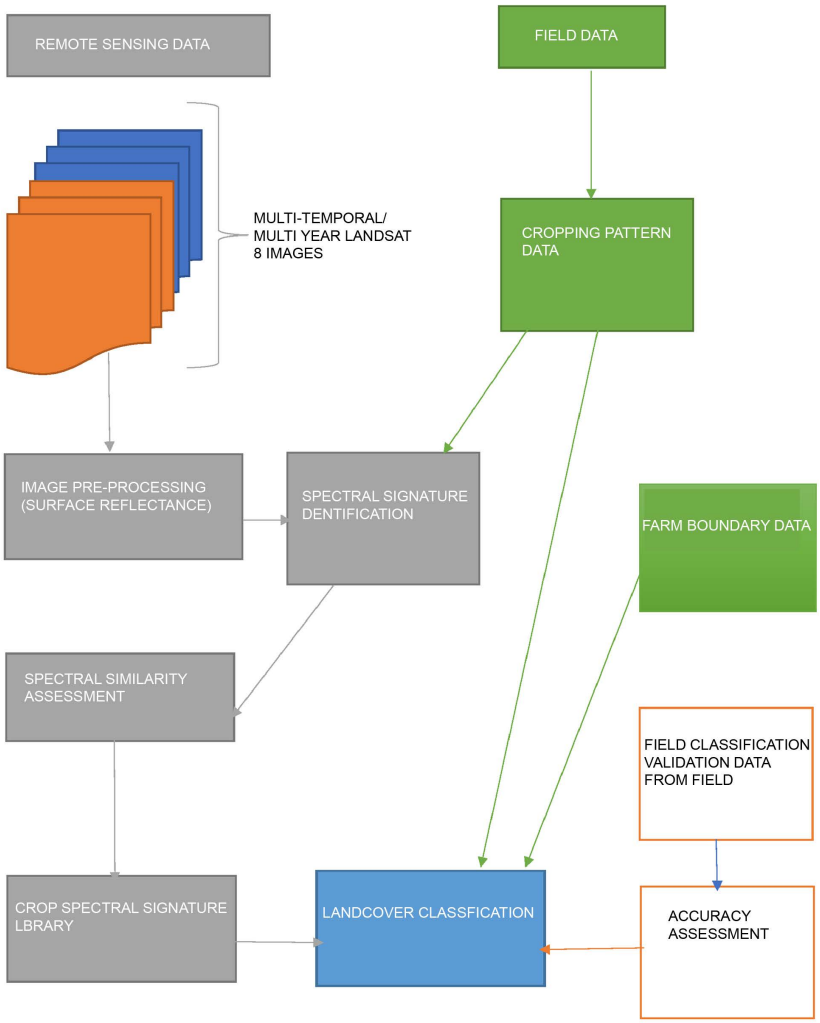

Figure 5. Methodology workflow.

2.7. Land Cover Accuracy Assessment

The error matrix evaluation method was found to be a valuable tool for assessing the accuracy results of the classification results; the error matrices were obtained by comparing the classification and the resulting ground-truth data collected from the field. The precision of classification was measured through the overall accuracy (OA) and Kappa (κ) indices, where OA is the ratio between correctly classified pixels and the total number of pixels, while κ index measures statistically the concordance between the ground truth data and classification values [52]. The Kappa coefficient was computed as follows.

$$k = \frac{\sum_{i=1}^{n} m_{i,i-} \sum_{i=1}^{n} (G_i C_i)}{N^2 - N \sum_{i=1}^{n} m_{i,i} - \sum_{i=1}^{n} (G_i C_i)} \quad (5)$$

where i is the class number N is the number of classified values compared to the true values, $m_{i,i}$ is the number of values belonging to the true class i that have also been classified as class i |9 normally at the diagonal area of the confusion matrix. C_i is the number of predicted values belonging to the class, i Gi is the total number of truth values belonging to the class. Once the Kappa coefficient is applied, it results in error of commission and omission. The error of commission gives a fraction of values predicted to be in the class but do not belong to that class, whilst the error of omission gives fraction of values belonging to a class but were predicted to be in a different class. Errors give producers and users precision, where the probability that a value in a given class was correctly classified is the producer's precision, while the probability that that a value predicted to be in a certain class actually is in that class is the user's precision.

3. Results

Changes in the short rain season (October-November-December) have been described by Recha *et al.* (2016) to start between mid-November and early December, thus causing changes in vegetative stages of the crop depending on the date of onset of rain. For data collected for five years, the vegetative stage of crop growth was found to occur between late December and February. In one unique case, while field data was collected, 2020 short rains began in early December, occasioning a two-month delay in the cropping calendar. These changes informed satellite imagery data acquisition for the years investigated. The graphs in **Figures 6-10** represent Variation of TOA reflectance for the 5 years that were examined in the study are for bands 2, 3, 4, 5, 6 and 7 for the various cropping patterns was eminent (**Figures 6-10**). The results represent the discrimination of the spectral signatures for the various cropping patterns extracted from the Landsat 8 data for each band used in the study. The focus of the result was to present the reflectance for the vegetative stage of growth for the various cropping patterns against the various bands used for the study, that is, bands 2, 3, 4, 5, 6 and 7 for the short rain seasons.

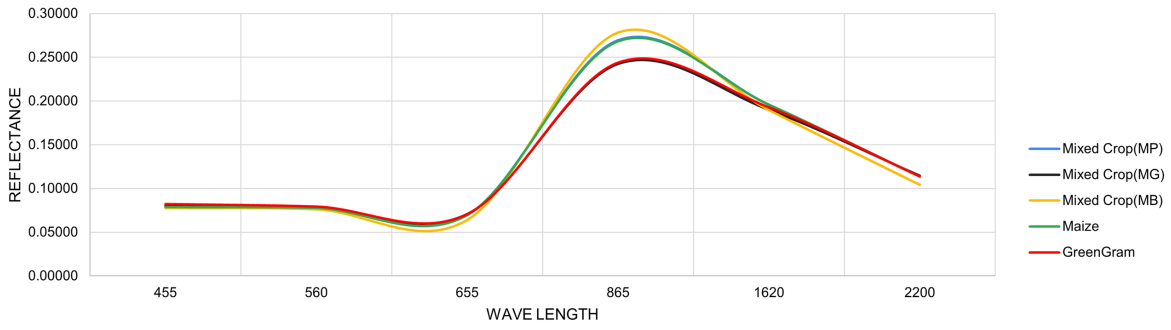

Figure 6. Landsat 8 TOA Spectral Reflectance for vegetative stage of growth for different crops in the 2015-short rain.

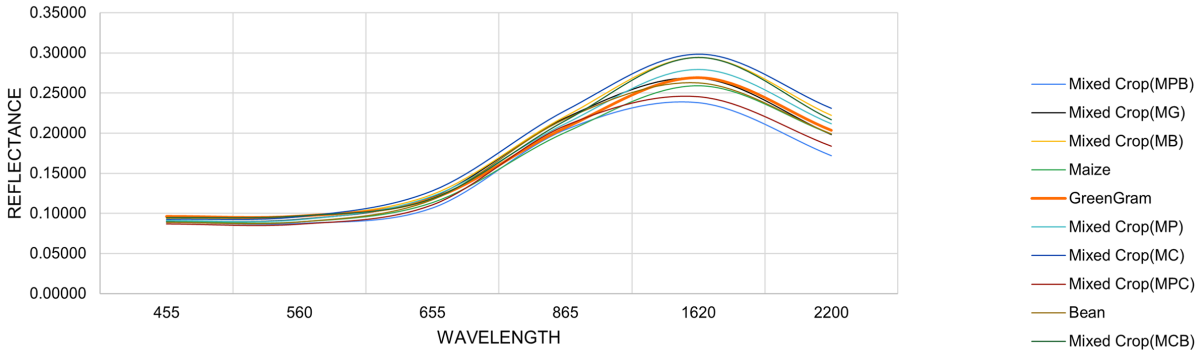

Figure 7. Landsat 8 TOA Spectral Reflectance for vegetative stage of growth for different crops in the 2018-short rain.

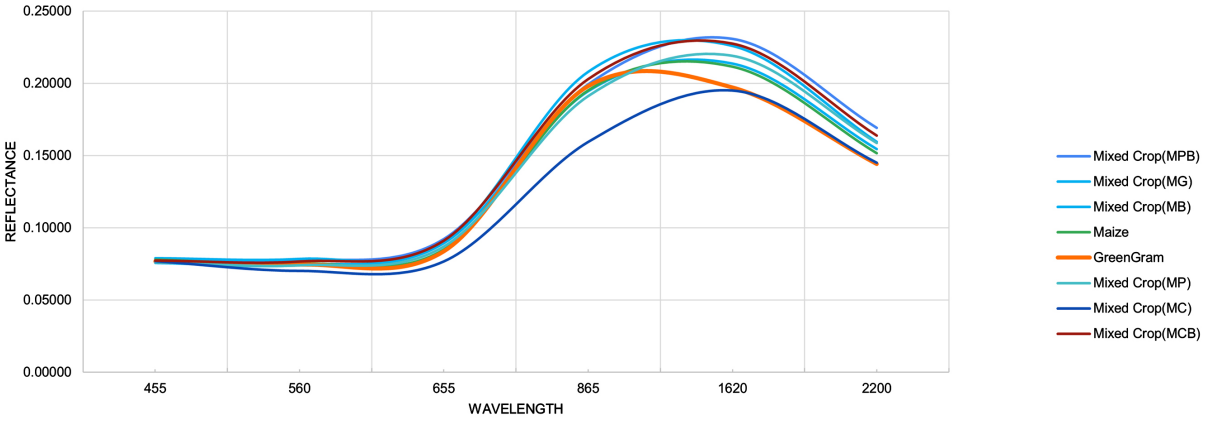

Figure 8. Landsat 8 TOA Spectral Reflectance for vegetative stage of growth for different crops in the 2017-short rain.

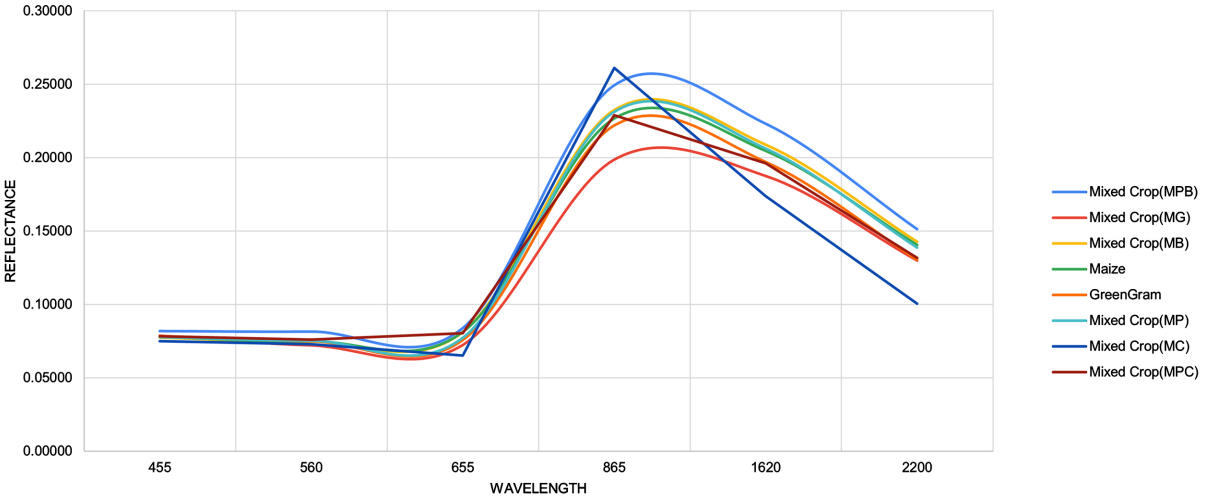

Figure 9. Landsat 8 TOA Spectral Reflectance for vegetative stage of growth for different crops in the 2015-short rains.

The results of the table show the levels of dissimilarity among the various cropping patterns for each of the TOA reflectance for each band (2, 3, 4, 5, 6, and 7). Table 5 and Table 6 depict the levels of similarity with a dissimilarity threshold of 0.95 in each of the cropping patterns.

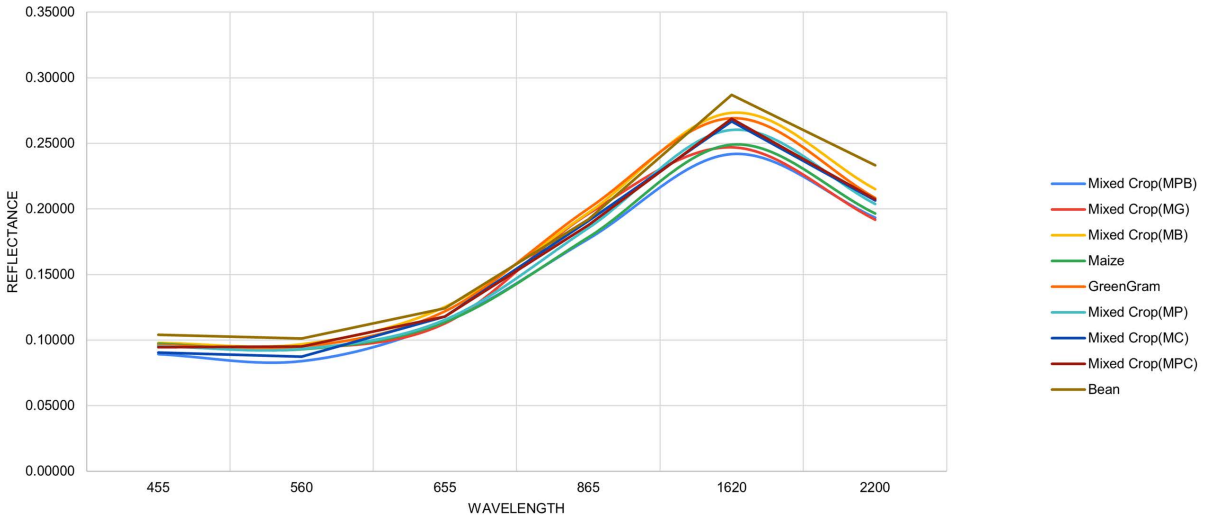

Figure 10. Landsat 8 TOA Spectral Reflectance for vegetative stage of growth for different crops in the 2013-short rains.

Table 5. Euclidean distance proximity matrix for all cropping patterns identified in the study area.

***Proximity matrix* (*Euclidean distance*):**										
	Mixed Crop (MPB)	Mixed Crop (MG)	Mixed Crop (MB)	Maize	GreenGram	Mixed Crop (MP)	Mixed Crop (MC)	Mixed Crop (MPC)	Bean	Mixed Crop (MCB)
***Mixed Crop* (*MPB*)**	0	0.259	0.288	0.278	0.257	0.280	0.059	0.221	0.344	0.337
***Mixed Crop* (*MG*)**	0.259	0	0.054	0.048	0.029	0.045	0.263	0.333	0.393	0.400
***Mixed Crop* (*MB*)**	0.288	0.054	0	0.037	0.042	0.027	0.292	0.365	0.440	0.443
Maize	0.278	0.048	0.037	0	0.036	0.017	0.284	0.350	0.425	0.424
GreenGram	0.257	0.029	0.042	0.036	0	0.033	0.261	0.333	0.407	0.418
***Mixed Crop* (*MP*)**	0.280	0.045	0.027	0.017	0.033	0	0.283	0.349	0.426	0.430
***Mixed Crop* (*MC*)**	0.059	0.263	0.292	0.284	0.261	0.283	0	0.182	0.323	0.354
***Mixed Crop* (*MPC*)**	0.221	0.333	0.365	0.350	0.333	0.349	0.182	0	0.243	0.397
Bean	0.344	0.393	0.440	0.425	0.407	0.426	0.323	0.243	0	0.319
***Mixed Crop* (*MCB*)**	0.337	0.400	0.443	0.424	0.418	0.430	0.354	0.397	0.319	0

Table 6. Dissimilarity threshold of 0.95 for cropping pattern TOA spectral reflectance.

List of similar objects (Dissimilarity threshold = 0.95):					
Object 1	Object 2	Dissimilarity	Object 1	Object 2	Dissimilarity
Mixed Crop (MPB)	Mixed Crop (MG)	0.259	Mixed Crop (MB)	Mixed Crop (MC)	0.292
Mixed Crop (MPB)	Mixed Crop (MB)	0.288	Mixed Crop (MB)	Mixed Crop (MPC)	0.365

Continued

Mixed Crop (MPB)	Maize	0.278	Mixed Crop (MB)	Bean	0.440
Mixed Crop (MPB)	GreenGram	0.257	Mixed Crop (MB)	Mixed Crop (MCB)	0.443
Mixed Crop (MPB)	Mixed Crop (MP)	0.280	Maize	GreenGram	0.036
Mixed Crop (MPB)	Mixed Crop (MC)	0.059	Maize	Mixed Crop (MP)	0.017
Mixed Crop (MPB)	Mixed Crop (MPC)	0.221	Maize	Mixed Crop (MC)	0.284
Mixed Crop (MPB)	Bean	0.344	Maize	Mixed Crop (MPC)	0.350
Mixed Crop (MPB)	Mixed Crop (MCB)	0.337	Maize	Bean	0.425
Mixed Crop (MG)	Mixed Crop (MB)	0.054	Maize	Mixed Crop (MCB)	0.424
Mixed Crop (MG)	Maize	0.048	GreenGram	Mixed Crop (MP)	0.033
Mixed Crop (MG)	GreenGram	0.029	GreenGram	Mixed Crop (MC)	0.261
Mixed Crop (MG)	Mixed Crop (MP)	0.045	GreenGram	Mixed Crop (MPC)	0.333
Mixed Crop (MG)	Mixed Crop (MC)	0.263	GreenGram	Bean	0.407
Mixed Crop (MG)	Mixed Crop (MPC)	0.333	GreenGram	Mixed Crop (MCB)	0.418
Mixed Crop (MG)	Bean	0.393	Mixed Crop (MP)	Mixed Crop (MC)	0.283
Mixed Crop (MG)	Mixed Crop (MCB)	0.400	Mixed Crop (MP)	Mixed Crop (MPC)	0.349
Mixed Crop (MB)	Maize	0.037	Mixed Crop (MP)	Bean	0.426
Mixed Crop (MB)	GreenGram	0.042	Mixed Crop (MP)	Mixed Crop (MCB)	0.430
Mixed Crop (MB)	Mixed Crop (MP)	0.027	Mixed Crop (MC)	Mixed Crop (MPC)	0.182

3.1. Green-Gram Spectral Signature Ranges for Bands 2, 3, 4, 5, 6 and 7

The graphs 11 to 16 represent the spectral signature ranges for green gram for each band evaluated individually in the study for 5 years. In **Figures 11-16** the spectral reflectance for green gram the were 0.07696 - 0.09632, 0.07466 - 0.9467, 0.0704047 - 0.12188, 0.19822 - 0.24387, 0.19269 - 0.26900 and 0.11354 - 0.20815 for Band 2, 3, 4, 5, 6, and 7. The identified ranges of spectral signature can be used to define the reflectance for green gram for agroecological zones IV and V for the vegetative stages of the crop growth during the short rains only (**Figures 11-16**). Similarities in the sigmoid curve of the TOA reflectance indicate that spectral signature reflectance were established through defined ranges for a particular cropping stage, season, and agroecological zones. **Figure 17** gives an overall comparison of all bands for the green gram for the selected 5-year period.

3.2. Landcover Classification and Accuracy Assessment

The classes selected in the land cover of the classification of the study area were mixed crop (maize and pigeon pea), mixed crop (maize and greengram), green gram, mixed crop (maize and beans), maize, built area, shrubland, mixed crop (maize and cowpea), beans and water. These classes were based on training data collected from the field. Classification was carried out using the TOA reflectance bands 2, 3, 4, 5, 6, and 7 of Landsat 8. The cropping pattern and farm boundary

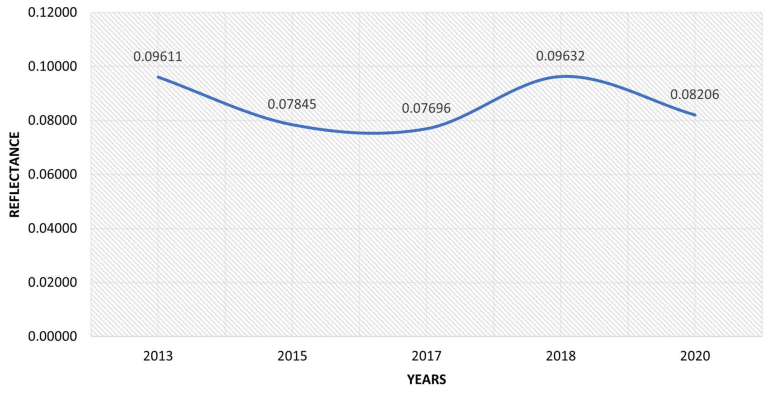

Figure 11. Greengram vegetative stage TOA reflectance for band 2.

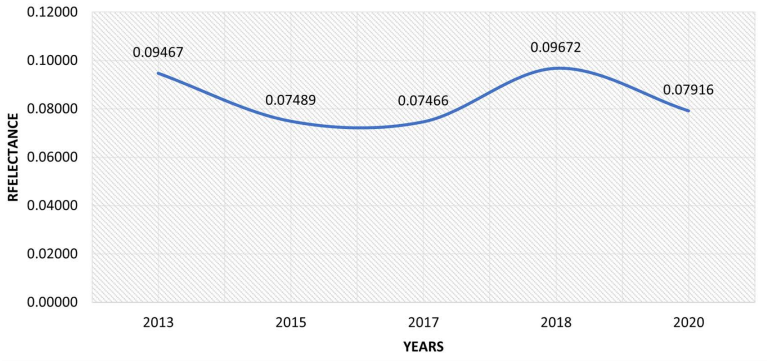

Figure 12. Greengram vegetative stage TOA reflectance for band 3.

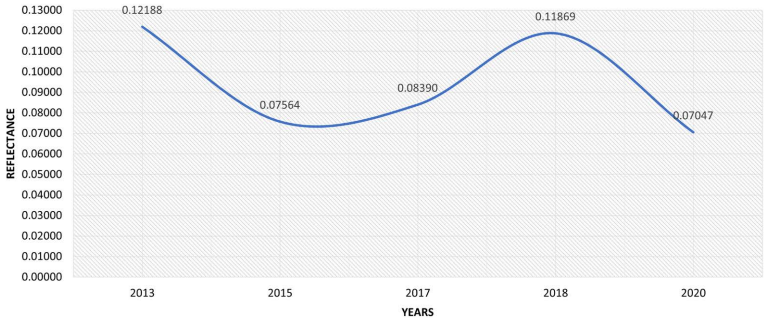

Figure 13. Greengram vegetative stage TOA reflectance for band 4.

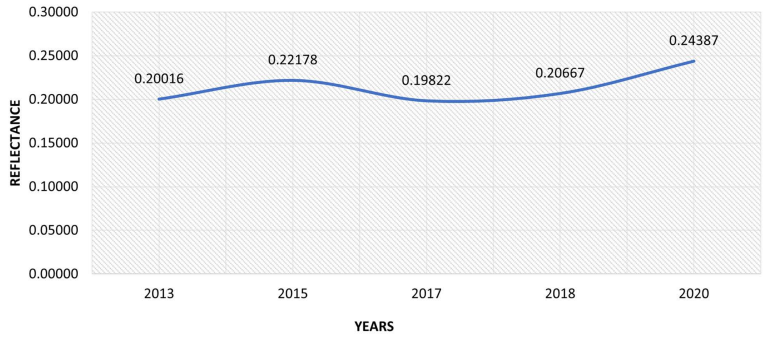

Figure 14. Greengram vegetative stage TOA reflectance for band 4.

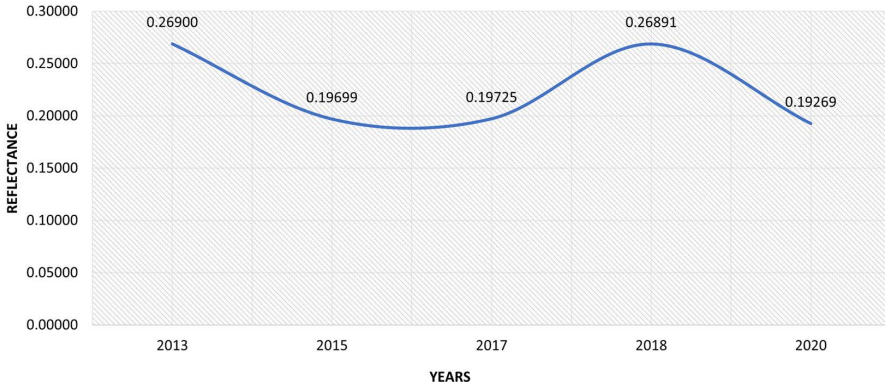

Figure 15. Greengram vegetative stage TOA reflectance for band 6.

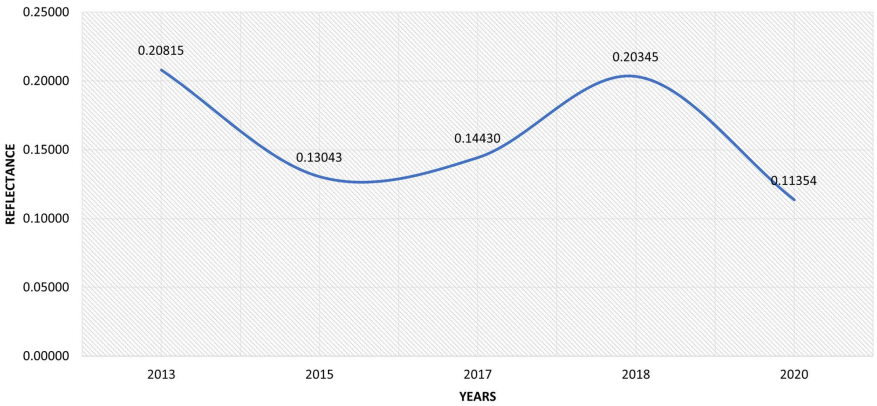

Figure 16. Greengram vegetative stage TOA reflectance for band 7.

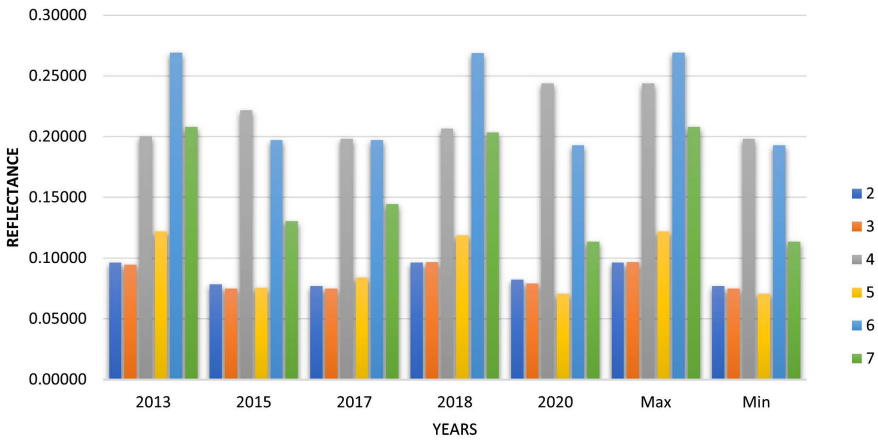

Figure 17. Greengram spectral signature library for all bands in a 5-year period.

data were used to improve the classification. The accuracy assessment of the land-cover classification of the study area was 84% with a kappa coefficient of 0.836 (Table 7). The producer accuracy and the user accuracy were 82.86% and 85.29%, respectively, for the green gram crop, other classes identified in the classification were; Mixed crop (maize and pigeon pea) 79.31% and 79.31%; Mixed crop (maize and green gram) 100% and 61.54%; Mixed crop (maize and beans) 88.89% and

70.59%; Maize 61.11% and 100%; Built up 92.86% and 92.86%; shrubland 83.33% and 90.91%; Mixed crop (maize and cowpea) 83.33% and 100%; Bean 100% and 100%; Water 100% and 100% for producers and users accuracy, respectively (Table 7) and the land cover classification (Figure 18).

Table 7. Landcover classification accuracy assessment using the confusion matrix.

Overall accuracy	= (143/171)	84%		
Kappa coefficient	0.83625731			
Class	Prod. Acc. (%)	User Acc. (%)	Prod. Acc. (Pixels)	User Acc. (Pixels)
Mixed crop (MP)	79.31	79.31	23/29	23/29
Mixed crop (MG)	100.00	61.54	8/8	8/13
Greengram	82.86	85.29	29/35	29/34
Mixed crop (MB)	88.89	70.59	24/27	24/34
Maize	61.11	100.00	11/18	11/11
Built-up area	92.86	92.86	13/14	13/14
Shrubland	83.33	90.91	10/12	10/11
Mixed crop (MC)	83.33	100.00	15/18	15/15
Bean	100.00	100.00	7/7	7/7
Water	100.00	100.00	3/3	3/3

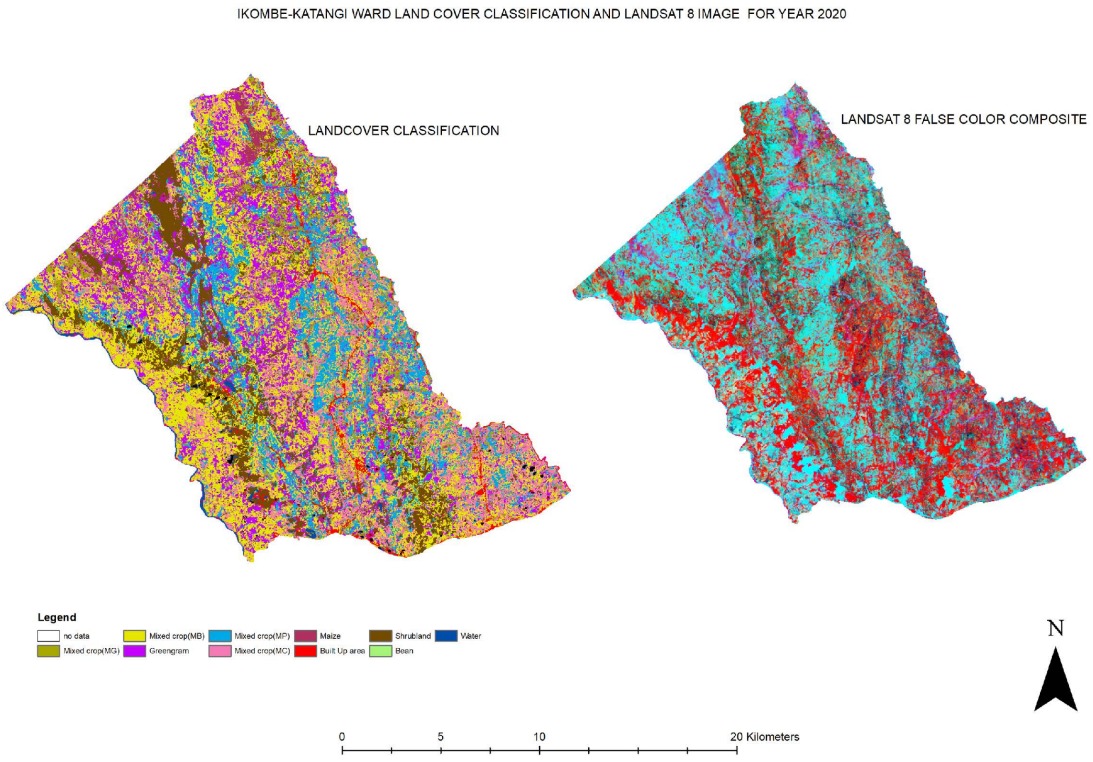

Figure 18. Ikombe-Katangi landcover classification using maximum likelihood classifier.

4. Discussion

Spectral resolution, which this study captures through the study of green gram spectral signatures affects the amount and type of thematic information available from a satellite scene for distinguishing vegetation (**Table 4**, **Figures 11-17**). This argument is in agreement with those of [53] who defined spectral resolution as the width of the spectral intervals (bands) used. Earth observation datasets have also proven to be effective in crop-type mapping and identification [54]. Furthermore [55] confirmed that satellite imagery data sets for crop identification ranged from low to high spatial resolutions. Multi-temporal Landsat data have been found to be very useful in crop monitoring. NASA Landsat-8 satellites provide images every 16 days with a spatial resolution of 30 m [56] [57]. Medium spatial resolution remote sensing data provide the spectral-temporal profiles of the crops of interest using a set of multispectral images acquired within a temporal period of time [57] [58]. Crop types have been distinguished using temporal and spectral characteristics of satellite images [58]-[60]. A study by [7] found that multitemporal imagery was very instrumental in the monitoring of crop growth stages of green gram enabling proper crop management such as irrigation, fertilization and pest control. [61] demonstrated the capabilities of Landsat 8 data integrated with sentinel 2 in enabling the understanding of the spatial variability of crop conditions.

A study by [23] has significantly proven the importance of various bands in a land cover classification that features other vegetation alongside crops. [62] suggested that the good performance of pre-processed OLI 8 satellite data in the classification of very fragmented agricultural landscapes. A calculation of TOA reflectance increased the probability of identification of cropping patterns in the study area **Table 4** and **Figures 6-10** especially with a focus on training data that had identified all possible cropping patterns. In addition, Existing data sets from USGS NASA for BOA provided results similar to those of TOA that were calculated for the images in question. Furthermore, a study by [63] indicated an agreement between ETM+ and OLI level 1 TOA reflectance within insitu measurement across all the spectral bands, whilst Level 2 reflectance products; Bottom of Atmosphere (BOA) decreased across the shorter wavelengths (bands 6 and 7) & for Landsat 8 across different landscape. [64] has shown that the use of surface reflectance and TOA produced validly accurate results in the estimation of LAI index. It is evident that in LAI, the atmospheric errors do not affect the resultant outputs. The use of TOA to avoid potential errors that can result from subsequent retrieval processes has been advocated for [65].

Differentiation of the different crops and crop patterns was possible, as indicated by the spectral similarity and showed the lowest dissimilarity index of 0.027 and the highest of 0.443 (**Table 5** and **Table 6**). An in-depth analysis of the spectral signatures associated with green gram for all bands **Figures 11-17** for various years investigated gives an indication of the possibilities of having spectral signature ranges for the identification of crops or cropping patterns in the field. Similar

findings to those reported with maize in our study were previously reported by [6] [66] conducted a multi-temporal analysis using Landsat 8 data to differentiate between rice and wheat in fragmented landscapes of South Asia. The research confirmed the capabilities to capture multiple phenological stages with Landsat 8 enhancing crop classification in regions with small, heterogeneous fields. [67] utilized Landsat 8 data for mapping smallholder farms in Sub-Saharan Africa. The research demonstrated accurate identification of different crop types within fragmented landscapes using Landsat 8 images. The need for accurate cropping pattern data and the demand for accurate and efficient crop pattern maps has been previously documented by [68]. Furthermore, [69] and [70] indicated that the spatial distribution and temporal dynamics of crop planting patterns have great contribution to the general understanding of agricultural production. Establishing these patterns is key towards mapping spectral signatures. In the study by [71] of various methods of spectral similarity assessment were used. The study highlighted the use of non-hybrid methods in the discrimination of objects with high level of similarity. [72] used the pearson correlation coefficient to check similarities between the NDVI time series and sentinel-2 data. Establishment of the area under the crop would also be possible. Comparison of spectral reflectance across the five years for the green gram showed that the range did not widen or had outliers but was significantly maintained across the bands. All spectral reflectance's of the green grams are compared over the years (**Figure 17**). High levels of similarity were observed for the vegetative stage of growth in the short rain season over the five years. This is confirmation of the potential of multispectral datasets for crop identification, as was discussed [8]. The precision in the identification of these crops is highly dependent on the stage of the crop, the agroecological zone where most of the climatic characteristics are similar and on the use of one cropping season as was the case for this particular study. This can be explained by the reports of [73] who showed that the spectral characteristics of crops were influenced by the chlorophyll and water content and, therefore, changes in the course of the growing season. The best results for crop identification may be achieved during the phase of full vegetation development, when the soil influence on the habitat's spectral reflectance is lowest. However, the exact time of the full development stages differ from crop to crop [73]. In this case, the study used the vegetative stage of green gram, where the crop was actively growing, when there was enough cover to reduce the influence of soil characteristics.

The problem in crop classification related to differences in spectral reflectance due to uneven crop maturation and differences in the growth phase of plants within a single field or among different surfaces (caused by other dates of sowing) is suggested by [74]. In our study, these challenges are addressed by mapping all possible cropping patterns and operating from one agroecological zone and one crop growth stage (when that stage is at its optimal level). This minimizes seasonal variation for the vegetative stage over the years. This particular methodology improves the homogeneity of the environment by taking care of several factors that

cause a heterogeneous nature in the identification of crops using satellite imagery. Our study spectral reflectance similarity findings as shown in **Figure 17** are in agreement with those of [75] who confirmed that identification of crops or detection of changes on agricultural surfaces is performed by multitemporal classification. As observed by [76] meteorological variables increase crop variation across region; therefore, our study focused on particular agroecological zones whose meteorological data showed a high level of similarity to overcome this challenge. In this case, our study worked with different dates in different years for the same cropping season while observing the planting date to determine satellite imagery data for use in the analysis. This was to ensure that all images were acquired when the crops were in the optimum vegetative stage of growth. In a similar approach, [60] used temporal signatures, agroclimatic diversity, and farm field sizes to enable crop classification. In our study, seasonality was found to be crucial as it affected the variability in time series, while regional stratification, for example, the use of agroecological zones, was found to give the best result. We showed that the classification of fragmented landscape land cover was improved using training data and farm boundaries, and these concurred with the findings by [60]. A further confirmation of crop identification is the landcover classification carried out in the study area are presented in **Figure 18**. The multi-approach to landcover classification, especially in cropland were in agreement with those of previous researchers [77]-[80] as a sure way of increasing the effectiveness of satellite imagery data of medium resolution in crop identification. Spectral reflectance range data for various crops can be generated using multitemporal and cropping pattern approaches for small-holder farms to increase crop identification. The application of spectral reflectance data for crop identification has revolutionized precision agriculture and agroecosystem management. According to [81] multi-temporal satellite data allows for monitoring crops throughout their growth stages optimizing agricultural practices. Further, data generated from spectral reflectance can be used for improving yield prediction accuracy through its combination with crop growth models, [48] In addition, [82] confirms the importance of spectral reflectance data in crop identification which is important for accurate crop maps that are crucial for land use planning and policymaking, ensuring sustainable agricultural development.

The overall accuracy in our study **Table 7** was 84% with the producer and user accuracy of 82.26% and 85.29%, respectively, for the green-gram crop in the landcover classification confirms these approaches capabilities in crop identification. Other cropping patterns whose identification was equivalently good was mixed crop (maize and pigeon pea), mixed crop (maize and beans), mixed crop (maize and cowpea) and bean whose producers and users precision were 79.31%, 79.31%, 88.89%, 70.59%, 83.33%, 100%, 100%, respectively. The evaluation of other classes such as maize was that 61% producers' accuracy and 100% users' accuracy. An indication that the identification of maize could have been influenced by its presence in other cropping patterns. [83] observed that mixed pixels reduce the impact

of mapping accuracy of land covers. Other classes were easily discriminated, and their precision was good (**Table 7**). The classification methodology differentiated other classes very well, where the built-up area and shrublands classes were well discriminated with producers and users accuracy of 92.86% and 92.86%; 83.33% and 90.9%, respectively. This research build on the need to develop spectral signature libraries in Africa with more research on different satellite datasets. The confirmation that greengram crop identification is a step towards the development of spectral signature libraries for Africa. Spectral signature libraries are designed for agricultural research purposes, such as the SPECCHIO Spectral online database maintained by the Remote Sensing Laboratories in the Department of Geography at the University of Zurich [84]. Although the study provides good classification accuracies, it is important to note that the use of multispectral datasets such as sentinel which is 10m could have provided better accuracies compared to Landsat 8 even though there were availability challenges for the phenological stage of growth that was investigated. [85] showcased the capabilities of sentinel-2 satellite imagery in classification which were far superior to Landsat 8. Nevertheless, combining Landsat 8 and sentinel-2 where datasets are available greatly improves classification accuracies, as reported by [23]. The importance of spectral matching of crop-specific spectral signatures' reflectance with insitu hyperspectral measurements is well suggested by [86]. The challenges of the absence of several multitemporal satellite data within and over years constrained rigorous investigation of other phenological stages of the crop.

Despite its advantages, using spectral reflectance data for crop identification presents various obstacles. These include the demand for high-quality, cloud-free images, the complexities of data processing, and the need for ground truth data for calibration and validation. Advanced machine learning methods and improved atmospheric correction approaches are being developed to solve these problems, improving the accuracy and usefulness of spectral reflectance data in agriculture [87].

5. Conclusions and Recommendations

We conclude that current methodologies used are reliably applicable to create a quasi-homogeneous environment in smallholder farms for the identification of crop types and cropping patterns. The use of a particular cropping season, within a target agroecological zone for a certain phenological stage of growth created the homogeneous environment required to work with medium-resolution data such as Landsat 8 in crop identification. The TOA reflectance improved the identification of crops, and the use of multi-temporal images was critical in creating spectral signature ranges for the crop identification. From the study there was no single spectral signature through which a particular crop exists, but most crops tended to oscillate within a specific range for all significant bands. Operating within an agroecological zone, certain crop stages and within a particular season were shown to be vital particularly if crop identification were to be successful for the

documentation of spectral signature ranges. The general effectiveness of this approach has been demonstrated by evaluating the accuracy of the land cover classification. This information can be used critically for the identification of crops. This will solve the challenges of monitoring of crops in fragmented smallholder farms, therefore enabling better decision making in enhancing crop productivity. Further, continuous crop identification and monitoring will Fasttrack the challenges of food security in Kenya and Africa at large. Utilizing spectral reflectance, can significantly have practical applications such optimizing field management practices to improving yield predictions and enhancing sustainable agricultural practices in mung bean production in Kenya.

This study recommends the use of similar approaches and a combination of Landsat 8 and sentinel-2 data, which have been documented to significantly increase precision. The approaches documented in the study can be used for local and national government planning through the provision of crop identification data. In addition, further research can be conducted to evaluate how other classification approaches perform with the spectral signatures generated from the Landsat 8 image for the study area. This is important especially where other multispectral satellite data may not be available.

Acknowledgement

Appreciation goes to the Kenya Climate Smart Crop Project under the Ministry of Agriculture, Livestock and Fisheries, Kenya, who were very instrumental in this study. An acknowledgement goes to Kenyatta University for the support provided in the execution of this research. The cooperative farmers of Ikombe-Katangi, who provided all the information that led to the success of the study.

Conflicts of Interest

The authors declare no conflicts of interest regarding the publication of this paper.

References

[1] Tittonell, P. and Giller, K.E. (2013) When Yield Gaps Are Poverty Traps: The Paradigm of Ecological Intensification in African Smallholder Agriculture. *Field Crops Research*, **143**, 76-90. https://doi.org/10.1016/j.fcr.2012.10.007

[2] Jayne, T.S., Mather, D. and Mghenyi, E. (2010) Principal Challenges Confronting Smallholder Agriculture in Sub-Saharan Africa. *World Development*, **38**, 1384-1398. https://doi.org/10.1016/j.worlddev.2010.06.002

[3] Fritz, S., Massart, M., Savin, I., Gallego, J. and Rembold, F. (2008) The Use of MODIS Data to Derive Acreage Estimations for Larger Fields: A Case Study in the South-Western Rostov Region of Russia. *International Journal of Applied Earth Observation and Geoinformation*, **10**, 453-466. https://doi.org/10.1016/j.jag.2007.12.004

[4] FAO. (2017) The Future of Food and Agriculture: Trends and Challenges. Rome.

[5] Tsiligirides, T.A. (1998) Remote Sensing as a Tool for Agricultural Statistics: A Case Study of Area Frame Sampling Methodology in Hellas. *Computers and Electronics in Agriculture*, **20**, 45-77. https://doi.org/10.1016/s0168-1699(98)00011-8

[6] Kumar, D.A., Srikanth, P., Neelima, T.L., Devi, M.U., Suresh, K. and Murthy, C.S. (2021) Monitoring of Spectral Signatures of Maize Crop Using Temporal SAR and Optical Remote Sensing Data. *International Journal of Bio-Resource and Stress Management*, **12**, 745-750. https://doi.org/10.23910/1.2021.2482

[7] Atzberger, C. (2013) Advances in Remote Sensing of Agriculture: Context Description, Existing Operational Monitoring Systems and Major Information Needs. *Remote Sensing*, **5**, 949-981. https://doi.org/10.3390/rs5020949

[8] Rembold, F., Meroni, M., Urbano, F., Royer, A., Atzberger, C., Lemoine, G., *et al*. (2015) Remote Sensing Time Series Analysis for Crop Monitoring with the SPIRITS Software: New Functionalities and Use Examples. *Frontiers in Environmental Science*, **3**, Article 46. https://doi.org/10.3389/fenvs.2015.00046

[9] Todoroff, P. and Kemp, J. (2016) Contribution of Remote Sensing to Crop Monitoring in Tropical Zones. In: Baghdadi, N. and Zribi, M., Eds., *Land Surface Remote Sensing in Agriculture and Forest*, Elsevier, 179-220. https://doi.org/10.1016/b978-1-78548-103-1.50005-4

[10] Ennouri, K. and Kallel, A. (2019) Remote Sensing: An Advanced Technique for Crop Condition Assessment. *Mathematical Problems in Engineering*, **2019**, Article 9404565. https://doi.org/10.1155/2019/9404565

[11] Chen, Z., Li, S., Ren, J., Gong, P., Zhang, M., Wang, L., *et al*. (2008) Monitoring and Management of Agriculture with Remote Sensing. In: Liang, S., Ed., *Advances in Land Remote Sensing*, Springer, 397-421. https://doi.org/10.1007/978-1-4020-6450-0_15

[12] Rao, N.R., Garg, P.K. and Ghosh, S.K. (2007) Development of an Agricultural Crops Spectral Library and Classification of Crops at Cultivar Level Using Hyperspectral Data. *Precision Agriculture*, **8**, 173-185. https://doi.org/10.1007/s11119-007-9037-x

[13] Galvão, L.S., Formaggio, A.R. and Tisot, D.A. (2005) Discrimination of Sugarcane Varieties in Southeastern Brazil with EO-1 Hyperion Data. *Remote Sensing of Environment*, **94**, 523-534. https://doi.org/10.1016/j.rse.2004.11.012

[14] Thenkabail, P.S., Gumma, M.K., Teluguntla, P. and Mohammed, I.A. (2014) Hyperspectral Remote Sensing of Vegetation and Agricultural Crops. *Photogrammetric Engineering and Remote Sensing*, **80**, 697-709.

[15] Makantasis, K., Karantzalos, K., Doulamis, A. and Doulamis, N. (2015) Deep Supervised Learning for Hyperspectral Data Classification through Convolutional Neural Networks. 2015 *IEEE International Geoscience and Remote Sensing Symposium* (*IGARSS*), Milan, 26-31 July 2015, 4959-4962. https://doi.org/10.1109/igarss.2015.7326945

[16] Pádua, L., Marques, P., Hruška, J., Adão, T., Peres, E., Morais, R., *et al*. (2018) Multi-temporal Vineyard Monitoring through UAV-Based RGB Imagery. *Remote Sensing*, **10**, Article 1907. https://doi.org/10.3390/rs10121907

[17] Wei, L., Wang, K., Lu, Q., Liang, Y., Li, H., Wang, Z., *et al*. (2021) Crops Fine Classification in Airborne Hyperspectral Imagery Based on Multi-Feature Fusion and Deep Learning. *Remote Sensing*, **13**, Article 2917. https://doi.org/10.3390/rs13152917

[18] Mariotto, I., Thenkabail, P. and Aneece, I. (2020) Global Hyperspectral Imaging Spec-tral-Library of Agricultural Crops for Central Asia. NASA EOSDIS Land Processes DAAC. https://doi.org/10.5067/Community/GHISA/GHISACASIA.001

[19] Krishna Mohan, B. and Porwal, A. (2015) Hyperspectral Image Processing and Analysis. *Current Science*, **108**, 833-841.

[20] Roumenina, E., Lachezar Filchev, L., Vassilev, V. and Dimitrov, P. (2012) Comparative

Analysis of Crop Maps for Selected Test Areas on the Territory of Bulgaria and Romania Using Simulated Proba-V and Spot Vegetation Data. *European Association of Remote Sensing LaboratoriesEARSeL eProceedings*, **11**, 155-160.

[21] Dusseux, P., Vertès, F., Corpetti, T., Corgne, S. and Hubert-Moy, L. (2014) Agricultural Practices in Grasslands Detected by Spatial Remote Sensing. *Environmental Monitoring and Assessment*, **186**, 8249-8265. https://doi.org/10.1007/s10661-014-4001-5

[22] Segarra, J., Buchaillot, M.L., Araus, J.L. and Kefauver, S.C. (2020) Remote Sensing for Precision Agriculture: Sentinel-2 Improved Features and Applications. *Agronomy*, **10**, Article 641. https://doi.org/10.3390/agronomy10050641

[23] Forkuor, G., Dimobe, K., Serme, I. and Tondoh, J.E. (2017) Landsat-8 vs. Sentinel-2: Examining the Added Value of Sentinel-2's Red-Edge Bands to Land-Use and Land-Cover Mapping in Burkina Faso. *GIScience & Remote Sensing*, **55**, 331-354. https://doi.org/10.1080/15481603.2017.1370169

[24] Rembold, F., Atzberger, C., Savin, I. and Rojas, O. (2013) Using Low Resolution Satellite Imagery for Yield Prediction and Yield Anomaly Detection. *Remote Sensing*, **5**, 1704-1733. https://doi.org/10.3390/rs5041704

[25] Palchowdhuri, Y., Valcarce-Diñeiro, R., King, P. and Sanabria-Soto, M. (2018) Classification of Multi-Temporal Spectral Indices for Crop Type Mapping: A Case Study in Coalville, UK. *The Journal of Agricultural Science*, **156**, 24-36. https://doi.org/10.1017/s0021859617000879

[26] Samant, T.K. (2014) Evaluation of Growth and Yield Parameters of Green Gram (*Vigna radiata* L.). *Agriculture Update*, **9**, 427-430. https://doi.org/10.15740/has/au/9.3/427-430

[27] Hargrave, B. (2006) Green Gram or Mung Beans (*Vigna radiata*). ECHO Development Notes no. 93.

[28] Purseglove, J.W. (2003) Tropical Crops. Longman.

[29] Hill, D.S. (1987) Agricultural Insect Pests of the Tropics and Their Control. Cambridge University Press.

[30] Wambua, J.M., Ngigi, M. and Lutta, M. (2017) Yields of Green Grams and Pigeonpeas under Smallholder Conditions in Machakos County, Kenya. *East African Agricultural and Forestry Journal*, **82**, 91-117. https://doi.org/10.1080/00128325.2017.1346903

[31] Malik, A., Fayyaz-Ul-Hassan, A., Abdul Wahieed, A., Qadir, G. and Asghar, R. (2006) Interactive Effects of Irrigation and Phosphorus on Green Gram (*Vigna radiata* L.). *Pakistan Journal of Botany*, **38**, 1119-1126.

[32] Singh, R.B., Kumar, P. and Woodhead, T. (2002) Smallholder Farmers in India: Food Security and Agriculture Policy. RAP Publication, 20-27.

[33] Mugo, J.W., Opijah, F.J., Ngaina, J., Karanja, F. and Mburu, M. (2020) Suitability of Green Gram Production in Kenya under Present and Future Climate Scenarios Using Bias-Corrected Cordex RCA4 Models. *Agricultural Sciences*, **11**, 882-896. https://doi.org/10.4236/as.2020.1110057

[34] Ogada, P. and Cigoja, D. (2017) Trends in Indigenous Crops Cultivation and Distribu-tion in Yatta Sub County, Kenya. *International Journal of Scientific & Engineering Research*, **8**, 480-483.

[35] Jiitzold, R. and Kutsch, H. (2000) Agro-Ecological Zones of the Tropics, with a Sample from Kenya. *Der Tropenlandwirt-Journal of Agriculture in the Tropics and Subtropics*, **83**, 15-34.

[36] Agesa, B., Onyango, C., Kathumo, V., Onwonga, R. and Karuku, G. (2019) Climate Change Effects on Crop Production in Kenya: Farmer Perceptions and Adaptation Strategies. *African Journal of Food, Agriculture, Nutrition and Development*, **19**, 14010-14042. https://doi.org/10.18697/ajfand.84.blfb1017

[37] Stafford, J.D., Reinecke, K.J., Kaminski, R.M. and Gerard, P.D. (2006) Multi-Stage Sampling for Large Scale Natural Resources Surveys: A Case Study of Rice and Waterfowl. *Journal of Environmental Management*, **78**, 353-361. https://doi.org/10.1016/j.jenvman.2005.04.029

[38] Cohen, L., Manion, L. and Morrison, K. (2017) Research Methods in Education, Routledge. https://doi.org/10.4324/9781315456539

[39] Morse, J.M. (2000) Determining Sample Size. *Qualitative Health Research*, **10**, 3-5. https://doi.org/10.1177/104973200129118183

[40] Shelestov, A., Lavreniuk, M., Kussul, N., Novikov, A. and Skakun, S. (2017) Exploring Google Earth Engine Platform for Big Data Processing: Classification of Multi-Temporal Satellite Imagery for Crop Mapping. *Frontiers in Earth Science*, **5**, Article 17. https://doi.org/10.3389/feart.2017.00017

[41] Agilandeeswari, L., Prabukumar, M., Radhesyam, V., Phaneendra, K.L.N.B. and Farhan, A. (2022) Crop Classification for Agricultural Applications in Hyperspectral Remote Sensing Images. *Applied Sciences*, **12**, Article 1670. https://doi.org/10.3390/app12031670

[42] Estévez, J., Vicent, J., Rivera-Caicedo, J.P., Morcillo-Pallarés, P., Vuolo, F., Sabater, N., *et al.* (2020) Gaussian Processes Retrieval of LAI from Sentinel-2 Top-of-Atmosphere Radiance Data. *ISPRS Journal of Photogrammetry and Remote Sensing*, **167**, 289-304. https://doi.org/10.1016/j.isprsjprs.2020.07.004

[43] Bruce, C.M. and Hilbert, D.W. (2004) Pre-Processing Methodology for Application to Landsat TM/ETM+ Imagery of the Wet Tropics. CSIRO Tropical Forest Research Centre and Rainforest CRC.

[44] Krishnan, R., Ramachandran, R., Murali Mohan, A., Radhadevi, P.V., Patra, S.K. and Chandrakanth, R. (1998) Satellite Data Preprocessing—New Perspectives. 90-98. http://www.isprs.org/proceedings/XXXII/part1/90_XXXII-part1.pdf

[45] USGS (2019) Landsat 8 (L8) Data Users Handbook. United States Geological Survey.

[46] Chander, G., Markham, B.L. and Helder, D.L. (2009) Summary of Current Radiometric Calibration Coefficients for Landsat MSS, TM, ETM+, and EO-1 ALI Sensors. *Remote Sensing of Environment*, **113**, 893-903. https://doi.org/10.1016/j.rse.2009.01.007

[47] Vishnu, S., Nidamanuri, R.R. and Bremananth, R. (2013) Spectral Material Mapping Using Hyperspectral Imagery: A Review of Spectral Matching and Library Search Methods. *Geocarto International*, **28**, 171-190. https://doi.org/10.1080/10106049.2012.665498

[48] Clevers, J.G.P.W. and Gitelson, A.A. (2013) Remote Estimation of Crop and Grass Chlorophyll and Nitrogen Content Using Red-Edge Bands on Sentinel-2 and -3. *International Journal of Applied Earth Observation and Geoinformation*, **23**, 344-351. https://doi.org/10.1016/j.jag.2012.10.008

[49] Richards, J.A. and Jia, X. (2006) Remote Sensing Digital Image Analysis. Springer.

[50] Hütt, C., Koppe, W., Miao, Y. and Bareth, G. (2016) Best Accuracy Land Use/Land Cover (LULC) Classification to Derive Crop Types Using Multitemporal, Multisensor, and Multi-Polarization SAR Satellite Images. *Remote Sensing*, **8**, Article 684. https://doi.org/10.3390/rs8080684

[51] Kavzoglu, T. and Reis, S. (2008) Performance Analysis of Maximum Likelihood and Artificial Neural Network Classifiers for Training Sets with Mixed Pixels. *GIScience & Remote Sensing*, **45**, 330-342. https://doi.org/10.2747/1548-1603.45.3.330

[52] Congalton, R.G. (1991) A Review of Assessing the Accuracy of Classifications of Remotely Sensed Data. *Remote Sensing of Environment*, **37**, 35-46. https://doi.org/10.1016/0034-4257(91)90048-b

[53] Jensen, J. R. (2000) Remote Sensing of the Environment: An Earth Resource Perspective. Pearson Prentice Hall.

[54] Castillejo-González, I.L., López-Granados, F., García-Ferrer, A., Peña-Barragán, J.M., Jurado-Expósito, M., de la Orden, M.S., *et al*. (2009) Object- and Pixel-Based Analysis for Mapping Crops and Their Agro-Environmental Associated Measures Using QuickBird Imagery. *Computers and Electronics in Agriculture*, **68**, 207-215. https://doi.org/10.1016/j.compag.2009.06.004

[55] Hong, G., Zhang, A., Zhou, F., Townley-Smith, L., Brisco, B. and Olthof, I. (2011) Crop-Type Identification Potential of Radarsat-2 and MODIS Images for the Canadian Prairies. *Canadian Journal of Remote Sensing*, **37**, 45-54. https://doi.org/10.5589/m11-026

[56] Immitzer, M., Vuolo, F. and Atzberger, C. (2016) First Experience with Sentinel-2 Data for Crop and Tree Species Classifications in Central Europe. *Remote Sensing*, **8**, Article 166. https://doi.org/10.3390/rs8030166

[57] Masialeti, I., Egbert, S. and Wardlow, B.D. (2010) A Comparative Analysis of Phenological Curves for Major Crops in Kansas. *GIScience & Remote Sensing*, **47**, 241-259. https://doi.org/10.2747/1548-1603.47.2.241

[58] Panigrahy, S., Ray, S.S., Manjunath, K.R., Pandey, P.S., Sharma, S.K., Sood, A., *et al*. (2011) A Spatial Database of Cropping System and Its Characteristics to Aid Climate Change Impact Assessment Studies. *Journal of the Indian Society of Remote Sensing*, **39**, 355-364. https://doi.org/10.1007/s12524-011-0093-3

[59] Heupel, K., Spengler, D. and Itzerott, S. (2018) A Progressive Crop-Type Classification Using Multitemporal Remote Sensing Data and Phenological Information. *PFG—Journal of Photogrammetry, Remote Sensing and Geoinformation Science*, **86**, 53-69. https://doi.org/10.1007/s41064-018-0050-7

[60] Arias, M., Campo-Bescós, M.Á. and Álvarez-Mozos, J. (2020) Crop Classification Based on Temporal Signatures of Sentinel-1 Observations over Navarre Province, Spain. *Remote Sensing*, **12**, Article 278. https://doi.org/10.3390/rs12020278

[61] Veloso, A., Mermoz, S., Bouvet, A., Le Toan, T., Planells, M., Dejoux, J., *et al*. (2017) Understanding the Temporal Behavior of Crops Using Sentinel-1 and Sentinel-2-Like Data for Agricultural Applications. *Remote Sensing of Environment*, **199**, 415-426. https://doi.org/10.1016/j.rse.2017.07.015

[62] Ouzemou, J., El Harti, A., Lhissou, R., El Moujahid, A., Bouch, N., El Ouazzani, R., *et al*. (2018) Crop Type Mapping from Pansharpened Landsat 8 NDVI Data: A Case of a Highly Fragmented and Intensive Agricultural System. *Remote Sensing Applications: Society and Environment*, **11**, 94-103. https://doi.org/10.1016/j.rsase.2018.05.002

[63] Teixeira Pinto, C., Jing, X. and Leigh, L. (2020) Evaluation Analysis of Landsat Level-1 and Level-2 Data Products Using in Situ Measurements. *Remote Sensing*, **12**, Article 2597. https://doi.org/10.3390/rs12162597

[64] Fang, H. and Liang, S. (2003) Retrieving Leaf Area Index with a Neural Network Method: Simulation and Validation. *IEEE Transactions on Geoscience and Remote*

Sensing, **41**, 2052-2062. https://doi.org/10.1109/tgrs.2003.813493

[65] Estévez, J., Berger, K., Vicent, J., Rivera-Caicedo, J.P., Wocher, M. and Verrelst, J. (2021) Top-of-Atmosphere Retrieval of Multiple Crop Traits Using Variational Heteroscedastic Gaussian Processes within a Hybrid Workflow. *Remote Sensing*, **13**, Article 1589. https://doi.org/10.3390/rs13081589

[66] Schneider, A., Mertes, C.M. and Formaggio, A.R. (2017) Discriminating between Rice and Wheat Crops Using Landsat 8 OLI Data. *International Journal of Remote Sensing*, **38**, 6046-6063.

[67] Deguise, I.E., Lefebvre, D. and Blondel, P. (2020) Crop Mapping of Smallholder Farms Using Landsat 8 Data in Sub-Saharan Africa. *Remote Sensing*, **12**, 957-968.

[68] Zhong, L., Hu, L., Yu, L., Gong, P. and Biging, G.S. (2016) Automated Mapping of Soybean and Corn Using Phenology. *ISPRS Journal of Photogrammetry and Remote Sensing*, **119**, 151-164. https://doi.org/10.1016/j.isprsjprs.2016.05.014

[69] Wu, W., Yu, Q., Peter, V.H., You, L., Yang, P. and Tang, H. (2014) How Could Agricultural Land Systems Contribute to Raise Food Production under Global Change? *Journal of Integrative Agriculture*, **13**, 1432-1442. https://doi.org/10.1016/s2095-3119(14)60819-4

[70] Yu, Q., Wu, W., Liu, Z., Verburg, P.H., Xia, T., Yang, P., *et al*. (2014) Interpretation of Climate Change and Agricultural Adaptations by Local Household Farmers: A Case Study at Bin County, Northeast China. *Journal of Integrative Agriculture*, **13**, 1599-1608. https://doi.org/10.1016/s2095-3119(14)60805-4

[71] Song, A., Choi, J., Kim, Y. and Kim, Y. (2015) Analysis of Appropriate Spectral Similarity Methods to Classify Target Species Using CASI Hyperspectral Images. 36*th Asian Conference on Remote Sensing*: *Fostering Resilient Growth in Asia*, Metro Manila, 24-28 October 2015, p. 3828.

[72] Vajsová, B., Fasbender, D., Wirnhardt, C., Lemajic, S. and Devos, W. (2020) Assessing Spatial Limits of Sentinel-2 Data on Arable Crops in the Context of Checks by Monitoring. *Remote Sensing*, **12**, Article 2195. https://doi.org/10.3390/rs12142195

[73] Vinciková, H., Hais, M., Brom, J., Procházka, J. and Pecharová, E. (2010) Landscape Studies Use of Remote Sensing Methods in Studying Agricultural Landscapes—A Review. *Journal of Landscape Studies*, **3**, 53-63.

[74] Nellis, M.D., Price, K.P. and Rundquist, D. (2009) Remote Sensing of Cropland Agriculture. In: Warner, T.A., Nellis, M.D. and Foody, G.M., Eds., *The SAGE Handbook of Remote Sensing*, SAGE Publications, Inc., 368-380. https://doi.org/10.4135/9780857021052.n26

[75] Hansen, J. (2004) Linking Dynamic Seasonal Climate Forecasts with Crop Simulation for Maize Yield Prediction in Semi-Arid Kenya. *Agricultural and Forest Meteorology*, **125**, 143-157. https://doi.org/10.1016/j.agrformet.2004.02.006

[76] Blickensdörfer, L., Schwieder, M., Pflugmacher, D., Nendel, C., Erasmi, S. and Hostert, P. (2022) Mapping of Crop Types and Crop Sequences with Combined Time Series of Sentinel-1, Sentinel-2 and Landsat 8 Data for Germany. *Remote Sensing of Environment*, **269**, Article 112831. https://doi.org/10.1016/j.rse.2021.112831

[77] Crnojevic, V., Lugonja, P., Brkljac, B. and Brunet, B. (2014) Classification of Small Agricultural Fields Using Combined Landsat-8 and Rapideye Imagery: Case Study of Northern Serbia. *Journal of Applied Remote Sensing*, **8**, Article 083512. https://doi.org/10.1117/1.jrs.8.083512

[78] Mtibaa, S. and Irie, M. (2016) Land Cover Mapping in Cropland Dominated Area Using Information on Vegetation Phenology and Multi-Seasonal Landsat 8 Images.

Euro-Mediterranean Journal for Environmental Integration, **1**, Article No. 6. https://doi.org/10.1007/s41207-016-0006-5

[79] Shi, X., Deng, Z., Ding, X. and Li, L. (2020) Land Cover Classification Combining Sentinel-1 and Landsat 8 Imagery Driven by Markov Random Field with Amendment Reliability Factors. *EURASIP Journal on Wireless Communications and Networking*, **2020**, Article No. 87. https://doi.org/10.1186/s13638-020-01713-5

[80] Ahady, A.B. and Kaplan, G. (2022) Classification Comparison of Landsat-8 and Sentinel-2 Data in Google Earth Engine, Study Case of the City of Kabul. *International Journal of Engineering and Geosciences*, **7**, 24-31. https://doi.org/10.26833/ijeg.860077

[81] Zhu, Z., Wang, S. and Woodcock, C.E. (2015) Improvement and Expansion of the Fmask Algorithm: Cloud, Cloud Shadow, and Snow Detection for Landsats 4-7, 8, and Sentinel 2 Images. *Remote Sensing of Environment*, **159**, 269-277. https://doi.org/10.1016/j.rse.2014.12.014

[82] Zhong, L., Hu, L. and Zhou, H. (2019) Deep Learning Based Multi-Temporal Crop Classification. *Remote Sensing of Environment*, **221**, 430-443. https://doi.org/10.1016/j.rse.2018.11.032

[83] Tariq, A., Yan, J., Gagnon, A.S., Khan, M.R. and Mumtaz, F. (2022) Mapping of Cropland, Cropping Pattern Patterns, and Crop Types by Combining Optical Remote Sensing Images with Decision Tree Classifier and Random Forest. *Geo-Spatial Information Science*, **26**, 302-320. https://doi.org/10.1080/10095020.2022.2100287

[84] Hueni, A., Nieke, J., Schopfer, J., Kneubühler, M. and Itten, K.I. (2009) The Spectral Database SPECCHIO for Improved Long-Term Usability and Data Sharing. *Computers & Geosciences*, **35**, 557-565. https://doi.org/10.1016/j.cageo.2008.03.015

[85] Hesping, M. (2020) Remote Sensing-Based Land Cover Classification and Change Detection Using Sentinel-2 Data and Forest Random Forest: A Case Study of Rusinga Island, Kenya. https://ep.liu.se/

[86] Rao, N.R. (2008) RETRACTED ARTICLE: Development of a Crop-Specific Spectral Library and Discrimination of Various Agricultural Crop Varieties Using Hyperspectral Imagery. *International Journal of Remote Sensing*, **29**, 131-144. https://doi.org/10.1080/01431160701241779

[87] Xie, Y., Sha, Z. and Yu, M. (2008) Remote Sensing Imagery in Vegetation Mapping: A Review. *Journal of Plant Ecology*, **1**, 9-23. https://doi.org/10.1093/jpe/rtm005